Metabolic Brain Disease (2019) 34:681–685
https://doi.org/10.1007/s11011-018-0375-3

SHORT COMMUNICATION

Evaluation strategy to determine reliable demyelination in the cuprizone model

Uta Chrzanowski[1] · Christoph Schmitz[1] · Anja Horn-Bochtler[2] · Anne Nack[1] · Markus Kipp[1,3]

Received: 6 October 2018 / Accepted: 19 December 2018 / Published online: 3 January 2019

Abstract

In multiple sclerosis patients, chronic clinical deficits are known to result from axonal degeneration which is triggered by inadequate remyelination. The underlying molecular mechanisms of remyelination and its failure remain currently unclear. In vivo models, among the cuprizone model, are valuable tools to study underlying mechanisms of remyelination and its failure. Since complete and reproducible demyelination of the analyzed brain region is an indispensable prerequisite for efficient remyelination experiments, in this study we systematically addressed which part of the corpus callosum is reliably and consistently demyelinated after acute cuprizone-induced demyelination. Following a novel evaluation strategy, we can show that at the level of the rostral hippocampus, the most medial sectors of the corpus callosum (spanning 500 μm in the horizontal plane) are consistently demyelinated, whereas more lateral sectors show inconsistent and incomplete demyelination. These results precisely define a part of the corpus callosum which should be used as a region of interest during remyelination experiments.

Keywords Cuprizone · Demyelination · Remyelination · Optical density · Regeneration

Introduction

Remyelination, which follows the pathological loss of myelin in diseases like Multiple sclerosis (MS), is a reparative process believed to ameliorate neurodegeneration. While remyelination occurs in many MS lesions (Prineas et al. 1993), it can become increasingly incomplete/inadequate or eventually it completely fails (Patrikios et al. 2006). Understanding why a relatively robust regenerative process should lose momentum is an important prerequisite for developing an effective therapeutic approach. One frequently applied preclinical model to study the effectiveness of drugs to boost remyelination is the cuprizone model (Slowik et al. 2015). The extent of de- and remyelination in this model is frequently determined by the semi-quantification of myelin protein expression via optical density measurements (Slowik et al. 2015; Werneburg et al. 2017). Commonly visualized myelin proteins are proteolipid protein (PLP), myelin associated glycoprotein (MAG), myelin basic protein (MBP) or 2',3'-cyclic-nucleotide 3'-phosphodiesterase (CNPase), and the analyzed region of interest is the midline of the corpus callosum at the level of the rostral hippocampus (*see* Fig. 1a). However, as recently demonstrated by our and other groups, demyelination is not spread evenly across the corpus callosum (Schmidt et al. 2013). Since consistent and reproducible demyelination is an indispensable prerequisite for efficient remyelination studies, the aim of this study was to analyze which part of the midline of the corpus callosum is consistently demyelinated and, therefore, should be used as a region of interest (ROI) in remyelination studies.

✉ Markus Kipp
markus.kipp@med.uni-rostock.de

[1] Department of Anatomy II, Ludwig-Maximilians-University of Munich, 80336 Munich, Germany

[2] Department of Anatomy I, Ludwig-Maximilians-University of Munich, 80336 Munich, Germany

[3] Institute of Anatomy, Rostock University Medical Center, Gertrudenstrasse 9, 18056 Rostock, Germany

Methods

Animals and cuprizone-induced demyelination

6–7 week-old C57BL/6 male mice (19 g - 20 g) were purchased from Janvier Labs (Le Genest-Saint-Isle, France). Microbiological monitoring was performed according to the Federation of European Laboratory Animal Science

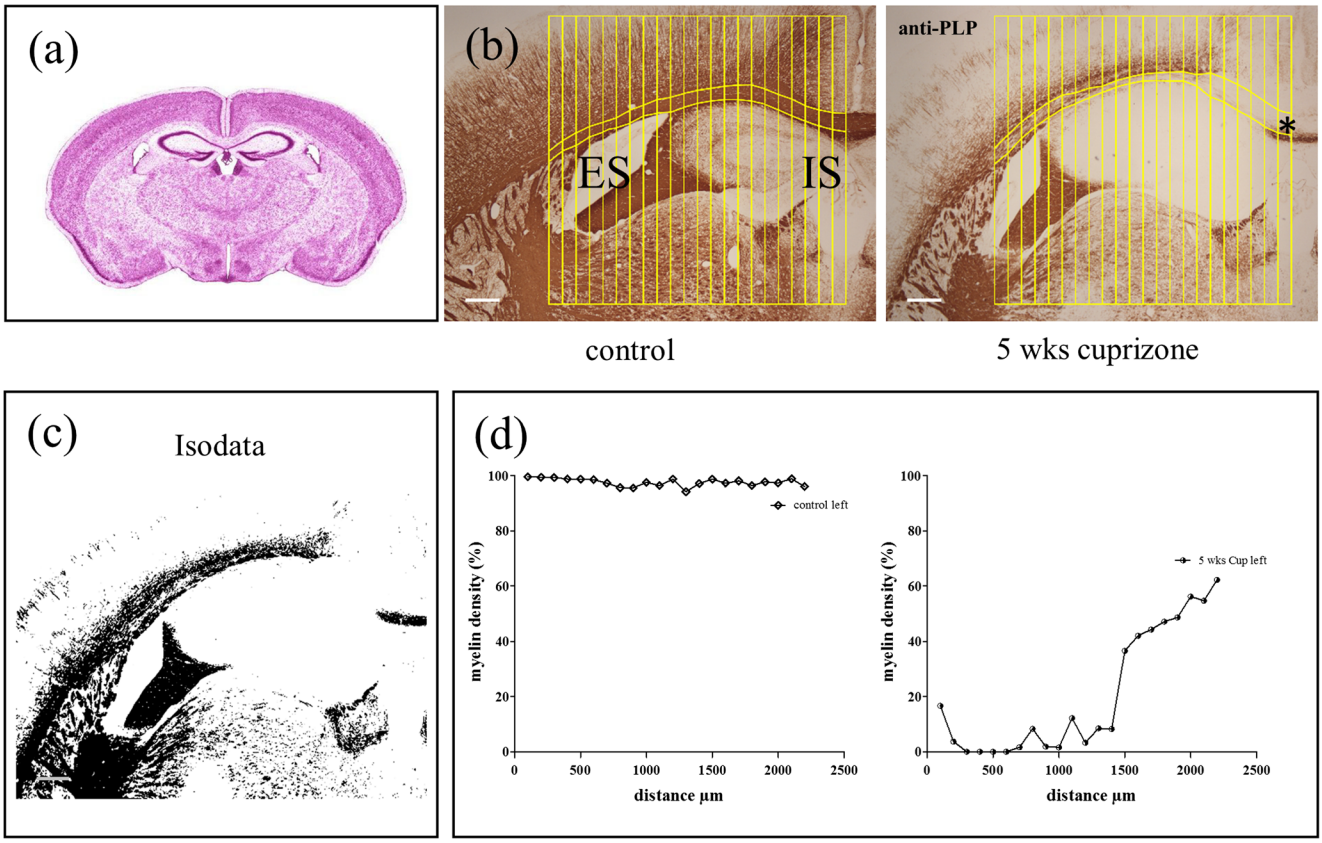

Fig. 1 **a** Brain level at which immunohistochemistry was performed. **b** Representative anti-PLP (proteolipid protein) stained section of a control and 5 weeks (wks) cuprizone (Cup)-intoxicated mouse. Corpus callosum sectors are outlined by the yellow columns. The star indicates the most internal corpus callosum sector. ES (external sector); IS (internal sector). **c** Representative illustration of a binary picture after thresholding using the *Isodata* algorithm provided by the ImageJ software package. **d** Representative result of staining intensity within the different corpus callosum sectors. 100 means a fully myelinated, zero a completely demyelinated corpus callosum sector. Each sector spans over a horizontal distance of 100 µm. Scale bars: (b/c) 250 µm

Associations recommendations. Experiments have been approved by the Regierung Oberbayern (reference number 55.2-154-2532-73-15) and conducted following guidelines of the Federation of European Laboratory Animal Science Associations (FELASA). Cuprizone-intoxication (0.25%) was performed as described previously for 1, 3 or 5 weeks (Hochstrasser et al. 2017). At the end of the experiment, mice were deeply anaesthetized with ketamine (100 mg·kg − 1 i.p.) and xylazine (10 mg·kg − 1 i.p.) and transcardially perfused with ice-cold PBS followed by a 3.7% paraformaldehyde solution (PFA; pH 7.4). Brains were subsequently dissected, embedded in paraffin, and then coronal sections (5 µm) were prepared.

Immunohistochemical evaluation

Established protocols were used for immunohistochemistry (Slowik et al. 2015). In brief, sections were rehydrated and, if necessary, antigens were unmasked with Tris/EDTA buffer (pH 9.0) or citrate (pH 6.0) heating. After washing in PBS, sections were incubated overnight (4 °C) with the primary antibodies diluted in blocking solution (serum of species in which the secondary antibody was produced). The following primary antibodies were used: anti-PLP (1:5000, Serotec, MCA839G; Puchheim, Germany), anti-MAG (1:4000, Abcam, ab89780; Cambridge, UK), anti-CNPase (1:2000, Abcam, ab6313; Cambridge, UK), and anti-MBP (1:500, Abcam, ab7349; Cambridge, UK). The next day, slides were incubated with biotinylated secondary antibodies (both 1:200, Vector Labs, Dossenheim, Germany; anti- mouse, BA9200; anti- rat, BA9400) for 1 h and then with peroxidase-coupled avidin-biotin complex (ABC kit; Vector Laboratories, Peterborough, UK) and treated with 3,3'-diaminobenzidine (DAKO, Hamburg, Germany) as a peroxidase substrate.

Fig. 2 **a** Anti-PLP (proteolipid protein), **b** anti-MAG (myelin associated glycoprotein) and **c** anti-CNPase (2',3'-cyclic-nucleotide 3'-phosphodiesterase) staining intensity in 22 corpus callosum sectors. 100 means a fully myelinated, zero a completely demyelinated corpus callosum sector. Each sector spans over a horizontal distance of 100 µm (blue line: first five sectors = 500 µm). Representative images from control, 1, 3 and 5 wks (weeks) cuprizone (Cup) intoxicated mice are shown on the right. * $p < 0.05$, ** $p < 0.01$ and *** $p < 0.001$; Mann Whitney test. Scale bars: (a-c) 250 µm

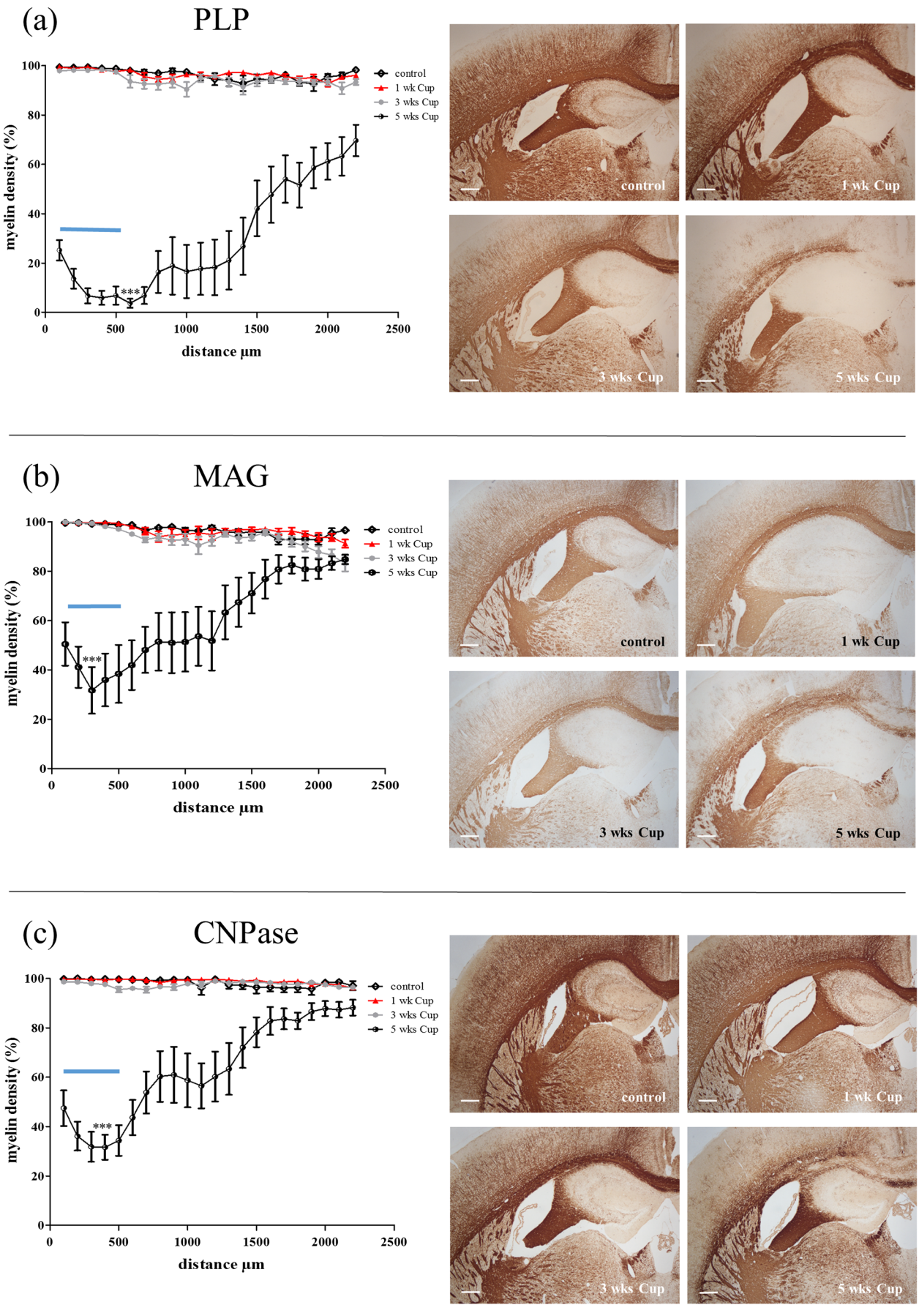
(a)
PLP
myelin density (%)
distance µm
control
1 wk Cup
3 wks Cup
5 wks Cup
***
(b)
MAG
myelin density (%)
distance µm
control
1 wk Cup
3 wks Cup
5 wks Cup
***
(c)
CNPase
myelin density (%)
distance µm
control
1 wk Cup
3 wks Cup
5 wks Cup
***

Stained sections were digitalized using a Nikon ECLIPSE E200 microscope (Nikon Instruments, Düsseldorf, Germany) equipped with a DS-2Mv camera.

Stained sections were evaluated by densitometry of the staining intensity using ImageJ and automated thresholding. To evaluate the reproducibility of cuprizone-induced demyelination in different sectors of the midline of the corpus callosum, the following strategy was followed: First, the midline of the corpus callosum was outlined, and then superimposed by a grid (distance between adjacent yellow lines = 100 μm, *see* Fig. 1b). After applying the *Isodata* threshold algorithm to obtain a binary image (*see* Fig. 1c), the optical density was measured in the individual fields, and subsequently blotted against the distance of the midline of the corpus callosum (star in Fig. 1b). Those parts of the corpus callosum near the midline are called "internal sectors" (IS in Fig. 1b) whereas those parts of the corpus callosum near the lateral ventricles are called "external sectors" (ES in Fig. 1b). Right and left hemispheres were separately evaluated, and results were averaged. A representative result of anti-PLP-processed slides from a control and 5 weeks cuprizone-intoxicated mouse is shown in Fig. 1d.

Statistics

Statistical analyses were performed using Prism 5 (GraphPad Software Inc., San Diego, CA, USA). All data are given as arithmetic means ± SEMs. A p value of <0.05 was considered to be statistically significant. Applied statistical tests are given in the respective figure legends. No outliers were excluded from the analyses. Kolmogorov-Smirnov test was applied to test for normal distribution of the data. Four control and five cuprizone animals (each time point) were used per experimental group.

Results

As demonstrated in Fig. 2, a homogenous anti-PLP, anti-MAG and anti-CNPase staining intensity was observed in all corpus callosum sectors of control and 1 week (wk) cuprizone-intoxicated mice. While similar results were obtained at week 3 for anti-PLP and anti-CNPase stained sections, a slight yet significant drop of anti-MAG staining intensity was observed in the external sectors of the corpus callosum midline. Statistical comparison using one-way ANOVA with the obtained p values corrected for multiple testing using Bonferronni's method revealed a significant loss of anti-MAG staining intensities within the four most external sectors compared to the most internal sector. At week 5, a significant loss of anti-PLP, anti-MAG, and anti-CNPase-staining intensities were evident in the internal sectors of the corpus callosum. The mean loss of myelin protein staining intensity within the five internal sectors was for PLP ~96% (control = 97.96 ± 0.74 versus 5 wks 3.69 ± 1.80 relative optical density; $p < 0.001$), for MAG ~68% (control = 99.22 ± 0.20 versus 5 wks 31.68 ± 9.46; $p < 0.001$), and for CNPase ~68% (control = 99.73 ± 0.14 versus 5 wks 31.64 ± 5.07; $p < 0.001$). Similar results were obtained for MBP ~62% (control = 98.76 ± 0.27 versus 5 wks 36.96 ± 6.15; $p < 0.001$; data not shown). Of note, the first five sectors, compromising a distance of 500 μm from the midline of the corpus callosum, showed most severe demyelination in all three applied immunohistochemical stains (blue lines in Fig. 2), whereas more lateral orientated sectors showed incomplete demyelination.

Discussion

In this study we addressed the reproducibility of demyelination within different corpus callosum subsectors. Following conventional protocols, acute demyelination is induced by a 5 weeks cuprizone intoxication period, and then pharmaceutical interventions are initiated to test for promyelinating drug effects (Slowik et al. 2015). Reproducible and preferably complete demyelination is an indispensable prerequisite for reliable remyelination studies (Stidworthy et al. 2003). Therefore, it is important to know which parts of the corpus callosum are demyelinated in a reproducible manner at week 5 before remyelination interventions are initiated. In vivo imaging methods are currently developed to visualize the myelination levels of the corpus callosum in living mice (Cao et al. 2018; de Paula Faria et al. 2014). Although such methods could help in the near future to monitor the efficacy of new drugs aimed at restoring myelin, their resolution is currently insufficient to visualize the extent of demyelination in corpus callosum subregions. Here, we show that demyelination is extensive and reproducible within the internal 500 μm spanning corpus callosum segments. Optical densities especially in anti-PLP stained sections show low standard error of the mean values. We, thus, recommend to focus on this callosal subregion during remyelination trials. Of note, this statement is true for the corpus callosum at the level of the rostral hippocampus. More rostral parts of the corpus callosum, such as at the level of the anterior commissure, might have a different demyelination pattern.

The observation that MAG- but not PLP- or CNPase-staining intensity was significantly reduced after 3 weeks of cuprizone intoxication is remarkable, although this finding has to be verified using other anti-myelin antibodies. It has been suggested that cuprizone-induced oligodendrocyte apoptosis mimics the pathology of so called "type-III MS lesions" (Lucchinetti et al. 2000). Such lesions are characterized by a selective reduction of MAG protein, and are reminiscent of virus- or toxin-induced demyelination rather than autoimmunity. Although further studies have to verify this observation,

selective early MAG loss in the cuprizone model further suggests that the mode of cuprizone-induced oligodendrocyte degeneration might well be relevant for MS.

Compliance with ethical standards

Conflict of interest The authors declare no competing financial interests.

Publisher's note Springer Nature remains neutral with regard to jurisdictional claims in published maps and institutional affiliations.

References

Cao J, Hu Y, Shazeeb MS, Pedraza CE, Pande N, Weinstock D, Polites GH, Zhang W, Chandross KJ, Ying X (2018) In vivo optical imaging of myelination events in a myelin basic protein promoter-driven luciferase transgenic mouse model. ASN Neuro 10: 1759091418777329. https://doi.org/10.1177/1759091418777329

de Paula Faria D, de Vries EF, Sijbesma JW, Dierckx RA, Buchpiguel CA, Copray S (2014) PET imaging of demyelination and remyelination in the cuprizone mouse model for multiple sclerosis: a comparison between [11C]CIC and [11C]MeDAS. Neuroimage 87:395–402. https://doi.org/10.1016/j.neuroimage.2013.10.057

Hochstrasser T, Exner GL, Nyamoya S, Schmitz C, Kipp M (2017) Cuprizone-containing pellets are less potent to induce consistent demyelination in the Corpus Callosum of C57BL/6 mice. J Mol Neurosci: MN 61:617–624. https://doi.org/10.1007/s12031-017-0903-3

Lucchinetti C, Bruck W, Parisi J, Scheithauer B, Rodriguez M, Lassmann H (2000) Heterogeneity of multiple sclerosis lesions: implications for the pathogenesis of demyelination. Ann Neurol 47:707–717

Patrikios P, Stadelmann C, Kutzelnigg A, Rauschka H, Schmidbauer M, Laursen H, Sorensen PS, Bruck W, Lucchinetti C, Lassmann H (2006) Remyelination is extensive in a subset of multiple sclerosis patients. Brain 129:3165–3172. https://doi.org/10.1093/brain/awl217

Prineas JW, Barnard RO, Kwon EE, Sharer LR, Cho ES (1993) Multiple sclerosis: remyelination of nascent lesions. Ann Neurol 33:137–151. https://doi.org/10.1002/ana.410330203

Schmidt T, Awad H, Slowik A, Beyer C, Kipp M, Clarner T (2013) Regional heterogeneity of cuprizone-induced demyelination: topographical aspects of the midline of the corpus callosum. J Mol Neurosci: MN 49:80–88. https://doi.org/10.1007/s12031-012-9896-0

Slowik A, Schmidt T, Beyer C, Amor S, Clarner T, Kipp M (2015) The sphingosine 1-phosphate receptor agonist FTY720 is neuroprotective after cuprizone-induced CNS demyelination. Br J Pharmacol 172:80–92. https://doi.org/10.1111/bph.12938

Stidworthy MF, Genoud S, Suter U, Mantei N, Franklin RJ (2003) Quantifying the early stages of remyelination following cuprizone-induced demyelination. Brain Pathol (Zurich, Switzerland) 13:329–339

Werneburg S, Fuchs HLS, Albers I, Burkhardt H, Gudi V, Skripuletz T, Stangel M, Gerardy-Schahn R, Hildebrandt H (2017) Polysialylation at early stages of oligodendrocyte differentiation promotes myelin repair. J Neurosci 37:8131–8141. https://doi.org/10.1523/jneurosci.1147-17.2017